GM-CSF but Not IL-17 Is Critical for the Development of Severe Interstitial Lung Disease in SKG Mice

Aoi Shiomi, Takashi Usui, Yuki Ishikawa, Masakazu Shimizu, Kosaku Murakami and Tsuneyo Mimori

J Immunol 2014; 193:849-859; Prepublished online 20 June 2014;
doi: 10.4049/jimmunol.1303255
http://www.jimmunol.org/content/193/2/849

The Journal of Immunology is published twice each month by
The American Association of Immunologists, Inc.,
9650 Rockville Pike, Bethesda, MD 20814-3994.

Print ISSN: 0022-1767 Online ISSN: 1550-6606.

GM-CSF but Not IL-17 Is Critical for the Development of Severe Interstitial Lung Disease in SKG Mice

Aoi Shiomi, Takashi Usui, Yuki Ishikawa, Masakazu Shimizu, Kosaku Murakami, and Tsuneyo Mimori

Interstitial lung disease (ILD) is a common complication and sometimes a prognostic factor of connective tissue diseases (CTDs) in humans. However, suitable animal model of severe CTD-associated ILD (CTD-ILD) has been limited. In this study, we showed that zymosan-treated SKG mice developed not only arthritis but also chronic–progressive ILD with high mortality over several months. The pathological and clinical features of ILD in zymosan-treated SKG mice were similar to that of human severe CTD-ILD. ILD in this mouse was characterized by massive infiltration of Th17 cells, GM-CSF–producing $CD4^+$ T cells, and $CD11b^+$ $Gr1^+$ neutrophils with fibrosis. Naive SKG T cells were skewed to differentiate into GM-CSF–producing cells, and GM-CSF secreted by T cells enhanced IL-6 and IL-1β production by macrophages, which in turn enhanced differentiation of IL-17A– and/or GM-CSF–producing T cells and infiltration of neutrophils into lung. Neutralization of GM-CSF completely blocked the development of this ILD, and the blocking of IL-6 signaling resulted in partial prevention of it, whereas neutralization of IL-17A did not. In contrast, the progression of arthritis was inhibited by the neutralization of GM-CSF and slightly by the neutralization of IL-17A, but not by the blocking of IL-6 signaling. These data suggested zymosan-treated SKG mice could be a useful mouse model of severe CTD-ILD, and GM-CSF, rather than IL-17A or IL-6, contributed to the development of ILD in zymosan-treated SKG mice, indicating that neutralization of GM-CSF would be a useful therapeutic strategy for severe CTD-ILD. ***The Journal of Immunology*****, 2014, 193: 849–859.**

Connective tissue diseases (CTDs) are systemic disorders that share certain clinical characteristics, including inflammation of the joints, serosal membranes, connective tissues, and blood vessels in various organs. The lung is a particularly vulnerable target organ of the CTDs, and 20–60% of CTDs complicates ILD (1). The CTD-associated interstitial lung disease (CTD-ILD) sometimes exhibits a severe and progressive ILD with high morbidity and mortality. Many ILDs are characterized by the accumulation of inflammatory cells within the lung, followed by the progressive deposition of extracellular matrix and the subsequent destruction of lung airspaces (2, 3). Analyses of inflammatory cells using bronchoalveolar lavage (BAL) of CTD-ILD patients showed an accumulation of neutrophils with or without increased percentages of lymphocytes (4, 5), and neutrophils were reported as important effector cells and associated with poor outcome of CTD-ILD (5–8). Immunohistochemical analysis of open lung biopsy specimens obtained from ILD patients also revealed that the density of plasma cells, neutrophils, macrophages, $CD3^+$, $CD4^+$, and $CD8^+$ T cells is significantly increased in the interstitium of ILD (3), and a previous report showed that the increased number of $CD4^+$ T cells in lung tissue was the characteristic of CTD-ILD (9). These reports suggested that not only lymphoid cells but also myeloid cells contribute to the pathogenesis of CTD-ILD. However, BAL and lung biopsy in patients with severe ILD are invasive and risky examinations; we still do not have enough information about severe ILD, and there are still many unknown mechanisms underlying the development of severe CTD-ILD. As a result of these difficulties, there have been few advancements in therapy for severe ILD for more than half a century. The major cause of these stagnations is the lack of suitable animal models for severe CTD-ILD. Although the pathogenesis of ILD has been investigated using animal models such as the murine bleomycin-induced pulmonary fibrosis model, most of these ILD models exhibit not progressive, but acute and transient disease (10). Moreover, most of the animal models are not related to autoimmunity, are fibrosis dominant, and do not fully recapitulate the histologic pattern of CTD-ILD (10). Therefore, it has been difficult to examine the entire pathogenesis of severe CTD-ILD and the effects of therapeutic interventions.

SKG mice, a mutant of the gene encoding ZAP70, spontaneously develop $CD4^+$ T cell–mediated autoimmune arthritis and also develop extra-articular manifestations, including ILD (11, 12). For this point, ILD in SKG mice could be a good candidate of a murine CTD-ILD model. However, the histological analyses in previous reports were not detailed, and the chronicity, prognosis, or etiology of ILD in SKG mice has yet to be clarified. The mutation of ZAP70 in SKG mice alters the sensitivity of T cells to positive and negative selection in the thymus, leading to production of potentially autoimmune T cells (11, 13). Injection of zymosan, a crude extract of β-glucans or purified β-glucans, activates innate immunity via TLR and Dectin-1 and drives differentiation and expansion of Th17 cells (14). In addition, complement activation

Department of Rheumatology and Clinical Immunology, Graduate School of Medicine, Kyoto University, Kyoto 606-8507, Japan

Received for publication December 4, 2013. Accepted for publication May 17, 2014.

This work was supported by Japan Society for the Promotion of Science Grants-in-Aid for Scientific Research 18591106 and 20591168 (to T.U.) and 18390290 and 22390201 (to T.M.).

Address correspondence and reprint requests to Dr. Takashi Usui, Department of Rheumatology and Clinical Immunology, Graduate School of Medicine, Kyoto University, 54-Kawahara-cho, Shogoin, Sakyo-ku, Kyoto 606-8507, Japan. E-mail address: takausui@kuhp.kyoto-u.ac.jp

The online version of this article contains supplemental material.

Abbreviations used in this article: BAL, bronchoalveolar lavage; CTD, connective tissue disease; ILD, interstitial lung disease; NSIP, nonspecific interstitial pneumonia; PAP, pulmonary alveolar proteinosis.

www.jimmunol.org/cgi/doi/10.4049/jimmunol.1303255

by β-glucans also contributes to promote Th17 differentiation in synergy with GM-CSF (15). These activated Th17 cells are reported to be responsible for the development of SKG arthritis, as adoptively transferred IL-17A$^{+/+}$ CD4$^+$ T cells did and IL-17A$^{-/-}$ CD4$^+$ T cells did not induce arthritis (13). In contrast, neutralizing IL-17 itself has proven to be a rather unsatisfactory method for blocking Th17 cell–mediated disease, giving only partial efficacy, which suggests that additional factors may be more important in Th17-mediated disease (16–18). Recent reports demonstrated that not IL-17A, but GM-CSF was critical for the pathogenesis of Th cells in experimental autoimmune encephalomyelitis, which had been known as a Th17-mediated disease (19, 20). Similarly, the other recent report showed CD4$^+$ T cell–derived GM-CSF contributed to inflammatory aortic aneurysms in a genetic model of Smad3 deficiency (21). Therefore, GM-CSF may also be a major contributor to triggering other autoimmune diseases previously known as Th17-mediated disease, such as SKG arthritis and/or its extra-articular manifestations.

In this study, we described that zymosan-treated SKG mice developed chronic–progressive and fatal ILD over several months. Because this ILD shared many histological characteristics with CTD-ILD and showed remarkable chronicity and severity, it is a useful model to understand severe CTD-ILD. Furthermore, we found that the blocking of IL-17A, GM-CSF, or IL-6 signals differently modified ILD and arthritis in this mouse. Among them, the neutralization of GM-CSF completely blocked the development of this ILD. These results suggested that the neutralization of GM-CSF would be a potential strategy for treatment of severe CTD-ILD.

Materials and Methods

Mice

SKG (CLEA Japan) and BALB/c mice (Japan SLC) at 7–12 wk were used. All mice were kept in specific pathogen-free conditions within the Institute of Laboratory Animals, Graduate School of Medicine, Kyoto University. All mice were treated in accordance with the guidelines for animal care approved by the Animal Experimentation Committee of Kyoto University (MedKyo 11052).

Induction of arthritis and ILD in SKG mice

Seven- to eight-week-old female mice were given a single i.p. injection of 7.5 mg/20 g body weight of zymosan (Sigma-Aldrich) suspended in 0.5 ml PBS or 0.5 ml PBS as a control, as previously described (14).

Clinical assessment of arthritis

Joint swelling was monitored by inspection and scored as follows: 0, normal; 1, mild, but definite redness and swelling of the ankle or wrist, or apparent redness and swelling limited to individual digits; 2, moderate redness and swelling of ankle or wrist; 3, severe redness and swelling of the entire paw, including digits; and 4, maximally inflamed limb with involvement of multiple joints. Clinical scores were represented as the total score of four paws.

Histology and histological score of the lung

The left lung and the other organs were inflated with 4% paraformaldehyde and paraffin embedded. Cryostat sections were stained with H&E and also subjected to Masson's trichrome staining. All images were captured using a Keyence BZ-9000. The severity of ILD was evaluated by measuring diffusely affected area, as previously reported (22). To score the mean of affected area with cellular infiltration precisely and exclude subjective assessment, three lung images per one mouse were randomly sampled, and all image processing was conducted by blinded method. The obtained lung images were converted to 8-bit grayscale, and the minimum and maximum points of the grayscale of each image were resettled 0 and 255 points, respectively, according to their histograms. The mean densities of the whole lung areas were then calculated by Image J software (Wayne Rasband). Each histological score of lung was described as the mean score of three images.

ELISA

Cytokines were measured by ELISA kits (eBioscience), according to the manufacturer's instructions. We confirmed that the existence of neutralizing/blocking Abs did not interfere with ELISA. To measure mouse anti-rat IgG Abs (Abs against anti-mouse GM-CSF Ab), the Coster 9018 ELISA plates were coated with 0.5 μg/ml rat anti-mouse GM-CSF Ab (eBioscience) in carbonate buffer and incubated overnight at 4˚C. Subsequently, the plate was washed with 0.05% Tween 20 containing PBS and blocked with assay diluent (eBioscience) for 1 h. Samples and mouse anti-rat IgG (H+L; Jackson ImmunoResearch Laboratories) as standards were diluted with assay diluent and added to the wells after washing. After 1-h incubation at room temperature, the plate was washed and 0.01 μg/ml peroxidase-conjugated F(ab′)$_2$ fragment of rabbit anti-mouse IgG Ab (Jackson ImmunoResearch Laboratories) was added as detection Ab and then incubated at room temperature for 1 h. After extensive washing, tetramethylbenzidine solution (eBioscience) was added, and, subsequently, 1 M H_3PO_4 was added to stop the reaction. The OD values at 550 nm were subtracted from those at 450 nm, and the values of samples were determined.

Isolation of lung-infiltrating cells

Mice were euthanized by exsanguination under chloroform-anesthesia, and then the lungs were perfused with PBS via hearts to remove blood cells. The right upper lobe was minced and digested in collagenase D (Roche Applied Science) for 30 min at 37˚C. Following digestion, 100 μl 100 mM EDTA was added and incubated for 5 min at 37˚C. Subsequently, digested lungs were filtered through a 100-μm nylon filter and the cells were collected.

Intracellular cytokine staining

Cell stimulation with PMA and ionomycin and intracellular cytokine staining were performed, as previously described (23). Pacific Blue–conjugated anti-CD3 (17A2), allophycocyanin-Cy7–conjugated anti-CD4 (RM4-5), PE-conjugated anti-F4/80 (CI:A3-1), allophycocyanin-conjugated anti–IL-17A (TC11-18H10.1), PE-Cy7–conjugated anti–IFN-γ (XMG1.2), PE-conjugated anti–IL-6 (MP5-20F3), and PE-conjugated anti–IL-4 (11B11) were purchased from BioLegend; PerCP-Cy5.5–conjugated anti-CD8 (53-6.7), PerCP-Cy5.5–conjugated anti-CD11b (M1/70), PE-Cy7–conjugated anti-CD45R (B220) (RA3-6B2), FITC-conjugated anti-Gr1 (RB6-8C5), FITC-conjugated anti–GM-CSF (MP1-22E9), and FITC-conjugated anti–TNF-α (MP6-XT22) were purchased from eBioscience. Data of flow cytometry were acquired on LSR Fortessa (BD Biosciences) and analyzed with FlowJo software (Tree Star).

Cell culture

We prepared single-cell suspensions of fresh splenocytes, and naive CD4$^+$ T cells were sorted by MACS CD4$^+$ T cell–negative selection (Miltenyi Biotec), followed by BD FACS Aria II (BD Biosciences) for CD4$^+$CD8$^-$ CD62L$^+$ cells. A total of 1.25×10^5 CD4$^+$CD62L$^+$ T cells was stimulated with 4 μg/ml anti-CD3 (2C11; eBioscience) and 5 μg/ml anti-CD28 (BioLegend) and cultured with 5 U/ml human rIL-2 (PeproTech) in 1:1 mixed medium of RPMI 1640 medium and DMEM supplemented with 10% FCS and 50 μM 2-ME, penicillin, and streptomycin for neutral condition (Th0), or with the following cytokines and neutralizing Abs for the desired polarization: IL-12 (1 ng/ml; PeproTech) and anti–IL-4 (20 μg /ml; eBioscience) for Th1 condition; IL-4 (50 ng/ml; Peprotech) and anti–IFN-γ (10 μg/ml; BioLegend) for Th2 condition; and IL-6 (20 ng/ml; BioLegend), TGF-β (10 ng/ml; WAKO), and anti–IFN-γ (10 μg/ml) for Th17 condition.

A total of 4×10^4 resident peritoneal macrophages was sorted by BD FACSAria II for forward light scatter^{high}, side light scatter^{high}, CD11b^{high} cells from lavage of the peritoneal cavity with 5 ml PBS with 2 mM EDTA and cultured with 100 ng/ml LPS (Sigma-Aldrich), 1 μg/ml zymosan (Sigma-Aldrich), and with or without GM-CSF (WAKO). In ex vivo culture, 1×10^6 fresh splenocytes were cultured with 5 μg/ml Con A, 5 μg/ml LPS, 10 μg/ml zymosan, or 100 μg/ml curdlan (Sigma-Aldrich).

Hydroxyproline measurement

The right middle lobe was homogenized in 1 ml PBS and centrifuged at 2000 rpm for 10 min. The supernatants were incubated with equal volume of 12 N HCl at 110˚C for 8 h. Then lung collagen levels were evaluated by quantifying hydroxyproline, as previously described (24).

Treatment study

Mouse anti-mouse IL-17A Ab, rat anti-mouse GM-CSF Ab, and their isotype Abs, mouse IgG1κ and rat IgG2aκ, respectively, were purchased

from eBioscience. SKG mice received 12 weekly i.p. injections of 100 μg these Abs or PBS from the day of zymosan injection. MR16-1 (rat anti-mouse IL-6R Ab) was provided by Chugai Pharmaceutical (Kanagawa, Japan). The isotype Abs of MR16-1, rat IgG1κ, were purchased from eBioscience. To prevent the production of anti–MR16-1 Ab, mice were i.p. injected with 2 mg MR16-1 on the day of zymosan injection, and then followed by 11 weekly i.p. injections of 0.5 mg MR16-1, as previously reported (25). After 12 wk, mice were euthanized and analyzed.

Statistical analysis

All analyses were performed using GraphPad Prism 5 software (GraphPad Software). The Mann–Whitney *U* test was performed for two-group comparisons. Kruskal Wallis test was performed for multiple group comparisons. Log-rank test was performed for analysis of survival curves. The p values <0.05 were considered statistically significant. Error bars in all figures indicate SEM; $*p < 0.05$, $**p < 0.01$, $***p < 0.001$.

Results

Zymosan-treated SKG mice develop chronic–progressive and fatal ILD over several months

We found that zymosan-treated SKG mice gradually lost their weight and showed progressive debilitation to death, and this was not observed in zymosan-treated BALB/c mice or PBS-treated SKG mice (Fig. 1A, 1B). Histological analysis revealed that zymosan-treated SKG mice at the terminal phase had severe ILD characterized by massive infiltration of inflammatory cells with massive fibrosis without honeycombing, which was not observed in zymosan-treated BALB/c mice (Fig. 1C, 1D). Although SKG mice were also reported to develop dermatitis and ileitis, the infiltration of inflammatory cells in these tissues and the other organs was mild (Fig. 1F, Supplemental Fig. 1). Time series analyses revealed the ILD in zymosan-treated SKG mice showed temporally uniform and chronic interstitial cellular infiltration with fibrosis, which started in peribronchovascular lesion and accompanied follicular bronchiolitis, which was commonly seen in CTD-ILD (26), in the early phase (Fig. 1E, 4 and 6 wk). These histological characteristics were in accordance with the nonspecific interstitial pneumonia (NSIP) in CTDs. In the later phase, the infiltration of inflammatory cells was gradually increased, and massive infiltration was extended to both peribronchiolar and alveolar spaces (Fig. 1E, 8 and 12 wk). The overlap of the histological pattern and the progressive exacerbation of ILD in this mouse also showed a marked similarity to CTD-ILD (27). The histological score of zymosan-treated SKG mice started to increase from the sixth week after zymosan injection and reached a peak at the twelfth week, but these changes were not observed in zymosan-treated BALB/c mice (Fig. 1G). Furthermore, increase of histological scores well correlated with the body weight losses and their elevated mortality (Fig. 1A, 1B, 1G). These findings indicated that the possible leading cause of death was respiratory failure by progression of ILD. Collectively, these results indicated that zymosan triggered chronic inflammatory cell infiltration into the lung and consequently developed chronic–progressive and fatal ILD, which had similar characteristics with severe CTD-ILD.

ILD in zymosan-treated SKG mice is characterized by the infiltration of IL-17A– or GM-CSF–producing T cells as well as CD11b$^+$Gr1$^+$ neutrophils

Next, we further investigated the characteristics of ILD in zymosan-treated SKG mice. After 18 wk from zymosan or PBS treatment, the histological scores of the lungs revealed marked increases in zymosan-treated SKG mice (Fig. 2A). The development of fibrosis in zymosan-treated SKG mice was confirmed by hydroxyproline estimation of lungs (Fig. 2B). The histological scores of zymosan-treated BALB/c mice also slightly increased compared with those of PBS-treated BALB/c mice; however, zymosan-treated SKG mice had statistically higher histological score compared with zymosan-treated BALB/c mice, and the pulmonary hydroxyproline level of zymosan-treated BALB/c mice was statistically not different from that of PBS-treated BALB/c mice (Fig. 2A, 2B). Infiltrated cell counts in lungs were measured by flow cytometry and revealed that zymosan-treated SKG mice had increased number of total cells, IL-17A–producing CD4$^+$ T cells, GM-CSF–producing CD4$^+$ T cells, and CD11b$^+$ Gr1$^+$ neutrophils compared with PBS-treated SKG mice. Notably, the majority of GM-CSF–producing CD4$^+$ T cells in zymosan-treated SKG mice are IL-17A–nonproducing (GM-CSF$^+$ IL-17A$^-$) cells, although a small number of GM-CSF/IL-17A–double-producing (GM-CSF$^+$ IL-17A$^+$) CD4$^+$ T cells is also increased (Fig. 2C, 2D). The number of CD4$^+$ T cells, CD11b$^+$Gr1$^-$ macrophages/monocytes, and IL-6–producing macrophages/monocytes (CD11b$^+$ Gr1$^-$ IL-6$^+$) of zymosan-treated SKG mice also tended to be higher than that of PBS-treated SKG mice, but they were not statistically significant. Some fractionations of lung-infiltrating cells in zymosan-treated BALB/c mice also seemed to be higher than those in PBS-treated BALB/c mice; however, it was not statistically significant except for the number of CD8$^+$ T cells. Serum IFN-γ and IL-6 were increased in zymosan-treated SKG mice compared with PBS-treated SKG mice. Serum IL-17A was also higher in zymosan-treated SKG but not statistically significant. Both serum GM-CSF and IL-4 were not detected in all groups (Fig. 2E). These results implied the possibility that IL-17A–producing CD4$^+$ T cells as well as GM-CSF–producing CD4$^+$ T cells, which may be distinct Th cells from Th17 cells, and IL-6–producing macrophages/monocytes contributed to the development of ILD in zymosan-treated SKG mice, and these upregulated cytokines contributed to neutrophil infiltration into the lung.

IL-6 and IL-1β production from macrophages of SKG and BALB/c mice is functionally equivalent

Zymosan is widely known as a strong activator of innate immunity and induces secretion of proinflammatory cytokines such as IL-6 or IL-1β by macrophages (28). Intraperitoneally injected zymosan is basically thought to activate residential peritoneal macrophages and then initiates systemic inflammatory process. The differentiation of Th17 cells is known to be driven by macrophage-derived IL-6 in SKG mice (15), and GM-CSF-production by CD4$^+$ T cells is reported to be regulated by inflammasome-derived IL-1β (29). However, because SKG mice are mutants of gene encoding ZAP70 in T cells, the ability of SKG macrophages to drive IL-17A– or GM-CSF–producing T cell differentiation itself is considered equivalent to that of BALB/c macrophages. Therefore, SKG T cells themselves must have a high potential to differentiate into IL-17A– or GM-CSF–producing cells. To assess this hypothesis, we analyzed the ability of macrophages from SKG and BALB/c mice to induce the differentiation of IL-17A– or GM-CSF–producing T cells. The FACS-sorted peritoneal macrophages of SKG or BALB/c mice were cultured with zymosan or LPS for 72 h, and the concentrations of IL-6 and IL-1β in the culture supernatants revealed there was no difference between SKG and BALB/c (Fig. 3A). We also analyzed the effect of GM-CSF at the various concentrations to enhance these cytokine productions from macrophages in the presence or absence of LPS or zymosan. Again, IL-6 and IL-1β productions of SKG and BALB/c macrophages were equally and significantly enhanced by GM-CSF (Fig. 3). Taken together, these results indicated that the differences of the phenotype of zymosan-treated SKG or BALB/c mice do not depend on the qualitative differences of their macrophages.

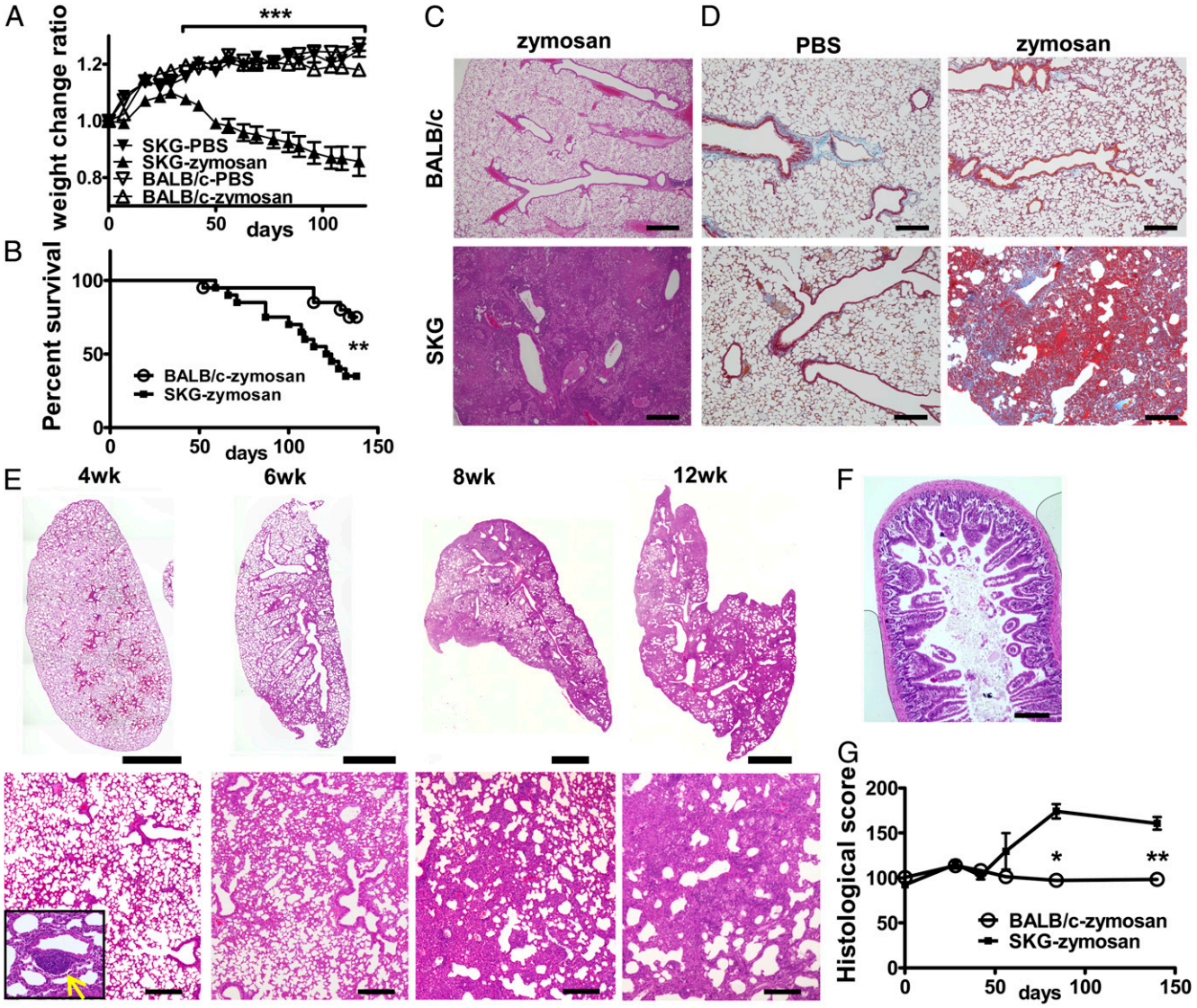

FIGURE 1. Zymosan-treated SKG mice develop chronic–progressive and severe ILD with high mortality. (**A**) The weight change ratio after i.p. injection of zymosan or PBS (PBS: $n = 5$, zymosan: $n = 30$). (**B**) The Kaplan–Meier survival analysis after injection of zymosan ($n = 20$). (**C**) H&E stain of the lung from zymosan-treated BALB/c mouse (*top*) and zymosan-treated SKG mouse (*bottom*) at 18 wk after zymosan treatment. Massive infiltrations of inflammatory cells were observed in zymosan-treated SKG mouse. Scale bar, 500 μm. (**D**) Masson's trichrome stain of the lung from PBS-treated BALB/c (*upper left*), PBS-treated SKG (*lower left*), zymosan-treated BALB/c (*upper right*), and zymosan-treated SKG (*lower right*) at 18 wk after zymosan or PBS treatment. Diffuse deposition of collagen fibers was observed in zymosan-treated SKG. Scale bar, 200 μm. (**E**) The time course of lung histology of SKG mice after zymosan injections. NSIP-like inflammatory cell infiltrations with follicular bronchiolitis (arrow) were observed in 4 and 6 wk, followed by massive infiltration of inflammatory cells in 8 and 12 wk after zymosan injections. Scale bar, 1.5 mm (*top*) and 250 μm (*bottom*). (**F**) H&E staining of small intestine from zymosan-treated SKG mouse at 18 wk after zymosan treatment. Scale bar, 200 μm. (**G**) The time course of lung histological score of zymosan-treated BALB/c or SKG mice after zymosan injections ($n = 5$). *$p < 0.05$, **$p < 0.01$, ***$p < 0.001$.

SKG T cells were skewed to differentiate into GM-CSF– or IL-17A–producing cells, and they are enhanced by macrophages

Freshly isolated splenic SKG CD4$^+$ T cells contained higher proportion of both GM-CSF–producing T cells and IL-17A–producing T cells (Fig. 4A). To compare the capacity of T cells to differentiate into IL-17A– or GM-CSF–producing T cells, FACS-sorted highly purified CD4$^+$CD62L$^+$ naive T cells from SKG or BALB/c mice were stimulated with anti-CD3 and anti-CD28 Abs for 5 d (neutral condition). FACS analyses of these T cells revealed that naive T cells from SKG mice differentiated into IL-17A–producing T cells or GM-CSF–producing T cells more preferentially than that from BALB/c mice (Fig. 4B). This result was confirmed by ELISA using culture supernatants of the same cells, although the difference of IL-17A concentration was not statistically significant (Fig. 4C). Moreover, SKG CD4$^+$ T cells are also prone to differentiate into IL-17A– or GM-CSF–producing T cells, even under Th1, Th2, or Th17 conditions, although there was no statistical difference between the frequency of GM-CSF–producing cells in SKG T cells and that in BALB/c T cells under the Th2 condition (Supplemental Fig. 2A, 2B). These results suggested that SKG CD4$^+$ T cells are primarily skewed to IL-17A– or GM-CSF–producing T cells both in vitro and in vivo. To further confirm these results, we cultured freshly isolated splenocytes from BALB/c or SKG mice with or without Con A, LPS, zymosan, or curdlan for 3 d to mimic in vivo conditions, and determined the concentration of IL-17A and GM-CSF in the supernatants by ELISA. As shown in Fig. 4D and 4E, SKG splenocytes produced higher amount of IL-17A and GM-CSF than BALB/c splenocytes

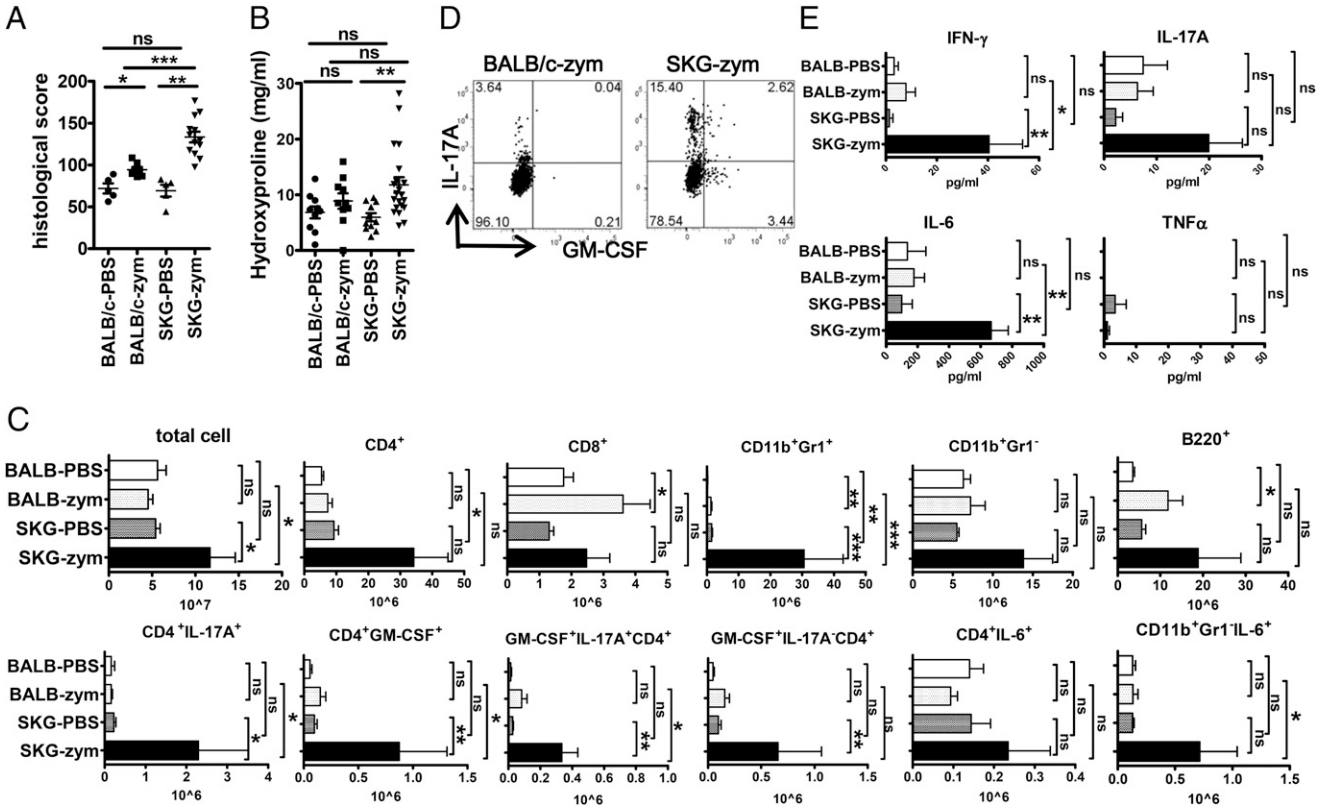

FIGURE 2. ILD in SKG mice was characterized by prominent infiltration of IL-17$^+$ CD4$^+$ T cells, GM-CSF$^+$ CD4$^+$ T cells, CD11b$^+$ Gr1$^+$ neutrophils, and pulmonary fibrosis. (**A**) Zymosan (zym)-treated SKG mice showed increased histological scores compared with zymosan (zym)-treated BALB/c mice and PBS-treated SKG mice at 18 wk after zymosan or PBS treatment (BALB/c-zym: $n = 7$, SKG-zym: $n = 13$, other groups: $n = 5$). (**B**) The concentrations of pulmonary hydroxyproline in PBS- or zymosan (zym)-treated SKG or BALB/c mice at 18 wk after zymosan or PBS treatment (SKG-zym: $n = 20$, other groups: $n = 10$). (**C**) Infiltrating cell counts in the lungs at 18 wk after zymosan or PBS treatment were measured by flow cytometry of dispersed cells from enzymatic lung digests. The numbers of total cells, CD4$^+$ T cells, CD8$^+$ T cells, CD11b$^+$ Gr1$^+$ neutrophils, CD11b$^+$ Gr1$^-$ macrophages/monocytes, B220$^+$ B cells, IL-17A–producing CD4$^+$ (CD4$^+$ IL-17A$^+$) T cells, GM-CSF–producing CD4$^+$ (CD4$^+$ GM-CSF$^+$) T cells, GM-CSF/IL-17A–double-producing CD4$^+$ (GM-CSF$^+$ IL-17A$^+$ CD4$^+$) T cells, GM-CSF–producing IL-17A–nonproducing CD4$^+$ (GM-CSF$^+$ IL-17A$^-$ CD4$^+$) T cells, IL-6–producing CD4$^+$ (CD4$^+$ IL-6$^+$) T cells, and IL-6–producing macrophages/monocytes (CD11b$^+$ Gr1$^-$ IL-6$^+$) were shown (BALB/c-PBS: $n = 5$, other groups: $n = 10$). (**D**) The majority of GM-CSF–producing CD4$^+$ T cells infiltrating in the lung of zymosan-treated SKG mouse were IL-17A–nonproducing cells. CD4$^+$ T cells infiltrating in lungs of zymosan-treated BALB/c and SKG mice at 18 wk after zymosan treatment were stained for intracellular IL-17A and GM-CSF. Representative results are shown ($n = 10$). (**E**) Serum concentrations of IFN-γ, IL-17A, IL-6, and TNF-α in BALB/c or SKG mice at 18 wk after zymosan or PBS treatment (PBS: $n = 5$, zymosan: $n = 15$). $^*p < 0.05$, $^{**}p < 0.01$, $^{***}p < 0.001$.

in response to Con A stimulation, but single stimulation by LPS, zymosan, or curdlan did not increase IL-17A or GM-CSF production in either BALB/c or SKG splenocyte cultures. However, costimulations of both T cells and non-T cells by Con A with LPS or zymosan or curdlan significantly amplified both IL-17A and GM-CSF productions. Furthermore, the concentrations of these two cytokines from SKG splenocytes were higher than that from BALB/c (Fig. 4D, 4E). These results in Fig. 4 and Supplemental Fig. 2 collectively indicate that SKG T cells differentiate into IL-17A– or GM-CSF–producing T cells more preferentially than BALB/c T cells. Although macrophages from SKG and BALB/c mice had no qualitative differences, GM-CSF promoted IL-6 and IL-1β production from them dose dependently, as shown in Fig. 3. Therefore, it appears that higher production of GM-CSF by SKG T cells promotes higher IL-6 and IL-1β production from macrophages, which in turn promotes further preferential differentiation and expansion of IL-17A– or GM-CSF–producing T cells. In conclusion, GM-CSF–secreting SKG T cells might be a key factor to exacerbate the vicious circle of IL-17A– or GM-CSF–producing T cell expansion.

Blocking of IL-17A, GM-CSF, or IL-6 signal differently modified ILD and arthritis of zymosan-treated SKG mice

We next examined the effect of blocking IL-17A, GM-CSF, or IL-6 signals on the development of ILD and arthritis in zymosan-treated SKG mice using their neutralization/blocking Abs. Each group of SKG mice received 12 weekly i.p. injections of either anti–IL-17A Ab, anti–GM-CSF Ab, anti–IL-6R Ab, or their isotype control Abs from the day of zymosan injection. Another group of SKG mice received 12 weekly i.p. injections of PBS instead of mAbs after zymosan injection as a control of isotype Abs, and showed that there was no statistical difference among weekly PBS-treated SKG group and all the isotype Ab-treated SKG groups in the weight change ratio, histological score, or pulmonary hydroxyproline level, indicating that these isotype control Abs are not pathogenic on their own (Supplemental Fig. 3). As shown in Fig. 5, GM-CSF neutralization completely prevented the weight loss (Fig. 5A, *middle*) and inhibited the progression of arthritis in zymosan-treated SKG mice (Fig. 5B, *middle*). In contrast, IL-17A neutralization did not suppress the weight loss but slightly suppressed the progression of arthritis in zymosan-treated SKG mice (Fig. 5A, 5B, *left*). Blocking of IL-6 signal weakly suppressed the weight loss (but it was not statistically significant) but did not affect the progression of arthritis in zymosan-treated SKG mice (Fig. 5A, 5B, *right*). Histological analysis after 12 injections revealed that GM-CSF neutralization and IL-6 signal blocking inhibited ILD progression in zymosan-treated SKG mice; however, IL-17A neutralization did not at all (Fig. 5C, 5D). The estimation of fibrosis by hydroxyproline confirmed these histological findings

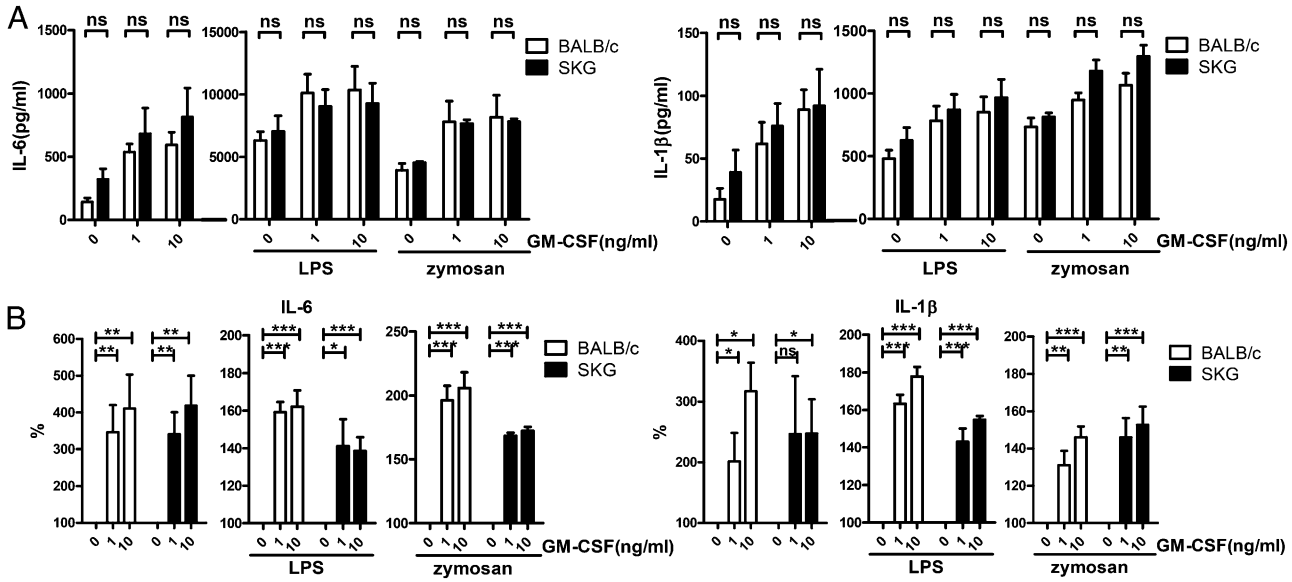

FIGURE 3. Cytokine production from macrophages of SKG mice was equivalent to that of BALB/c mice and enhanced by GM-CSF. (**A**) Peritoneal CD11b$^+$ macrophages were cultured for 3 d with or without 100 ng/ml LPS or 1 μg/ml zymosan in the presence of GM-CSF at indicated doses. IL-6 and IL-1β in the supernatant were measured by ELISA ($n = 5$). (**B**) Percentage of changes of cytokine concentrations shown in (A) from cultures without GM-CSF ($n = 5$). $*p < 0.05$, $**p < 0.01$, $***p < 0.001$.

(Fig. 5E). These results demonstrated that IL-17A, GM-CSF, and IL-6 have different roles in ILD and arthritis of zymosan-treated SKG mice, and that GM-CSF and IL-6 were more potent molecular targets to treat ILD in this mouse than IL-17A.

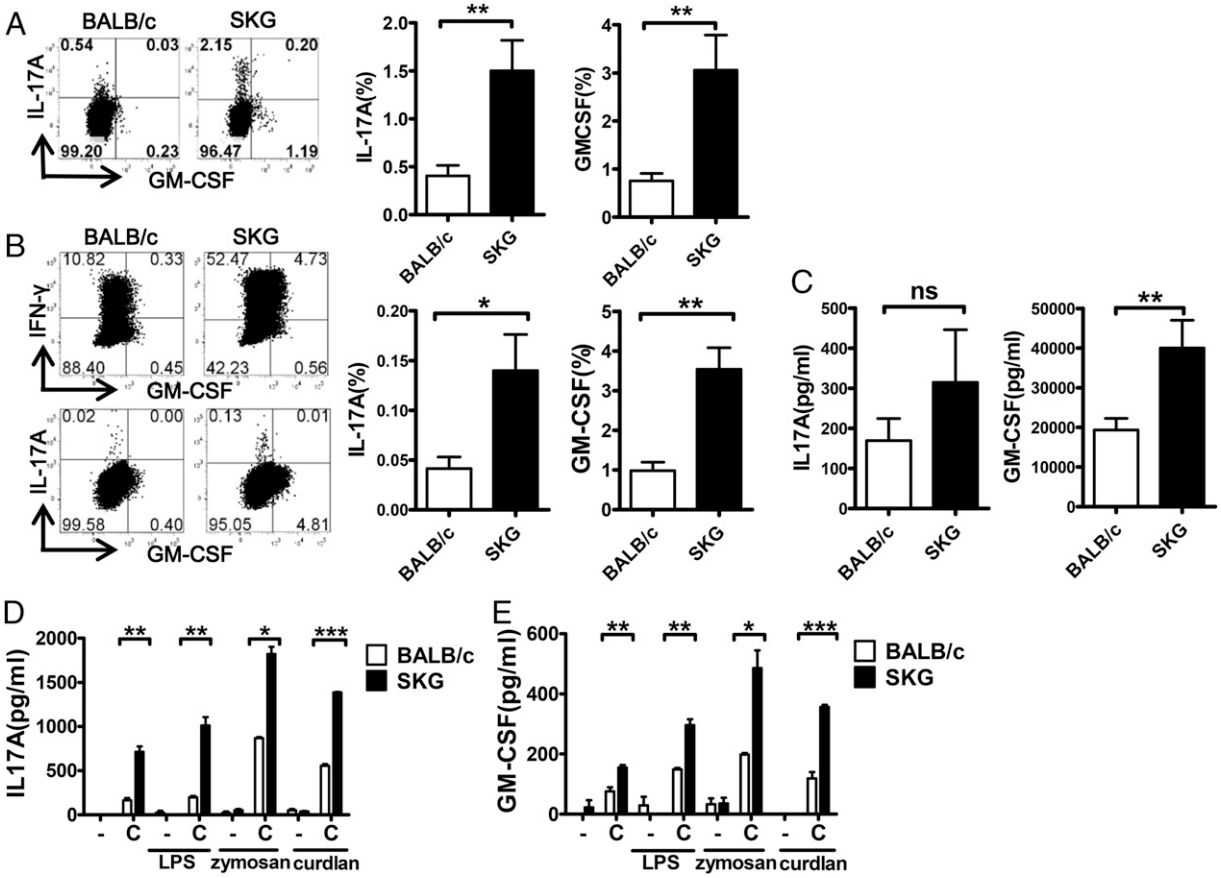

FIGURE 4. SKG T cells were skewed to differentiate into IL-17A– and GM-CSF–producing cells. (**A**) Freshly isolated BALB/c or SKG splenic CD4$^+$ T cells were stained for intracellular IL-17A and GM-CSF. Representative results are shown ($n = 8$). (**B** and **C**) FACS-sorted CD4$^+$ CD62L$^+$ naive T cells of SKG and BALB/c mice were cultured under the stimulation of anti-CD3/28 Abs. At day 5, cultured cells were analyzed by FACS (B), or restimulated with PMA/ionomycin for 24 h, and the concentrations of IL-17A and GM-CSF in the culture supernatants were determined by ELISA (C). Representative results are shown ($n = 5$). (**D** and **E**) Freshly isolated BALB/c or SKG splenocytes were cultured with or without Con A (C), LPS, zymosan, or curdlan for 3 d, and the concentrations of IL-17A (D) and GM-CSF (E) in the supernatants were measured by ELISA ($n = 3$). $*p < 0.05$, $**p < 0.01$, $***p < 0.001$.

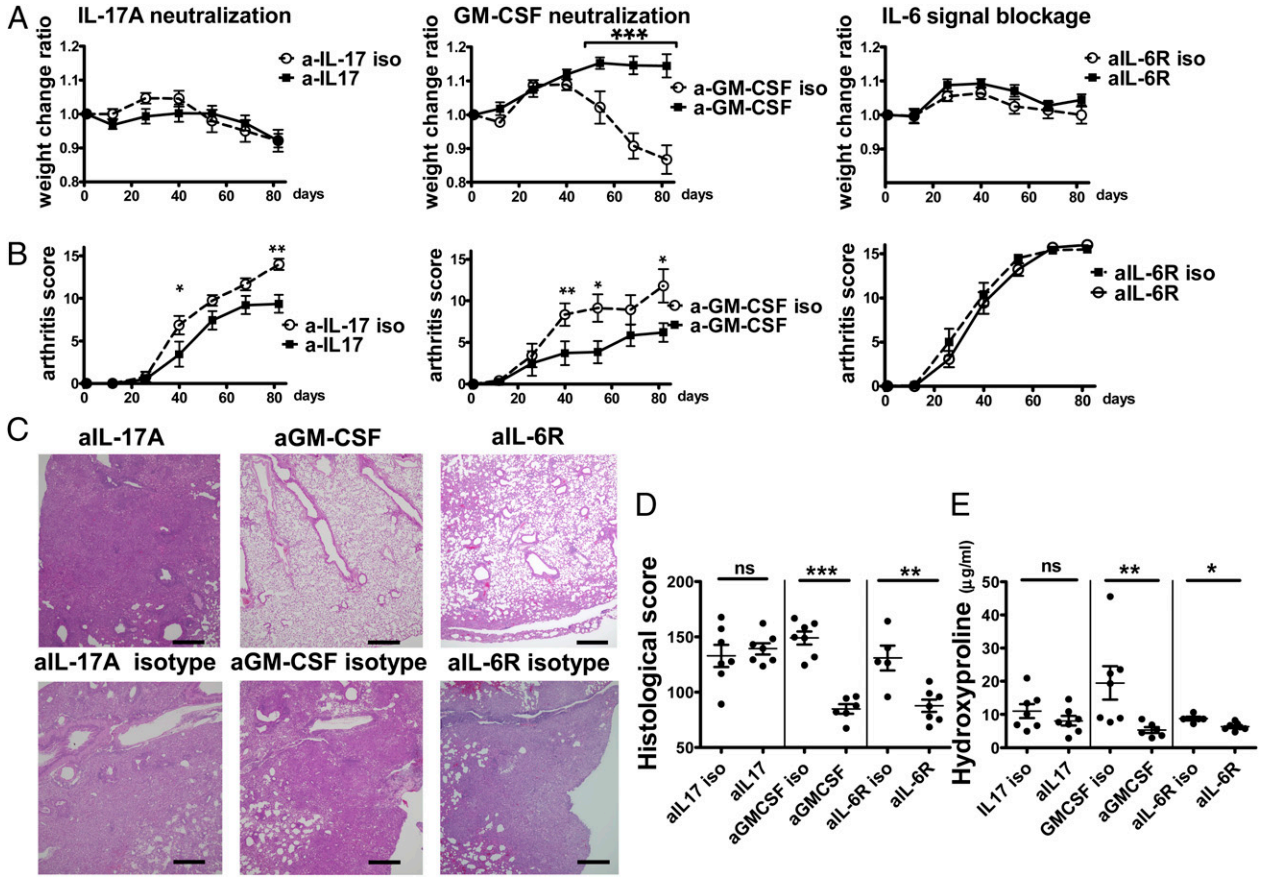

FIGURE 5. GM-CSF neutralization inhibited the development of ILD in SKG mice. (**A** and **B**) Weight change ratio (A) and arthritis score (B) of SKG mice that received a single i.p. injection of zymosan and 12 weekly i.p. injections of anti–IL-17A Ab (*left*), anti–GM-CSF Ab (*middle*), anti–IL-6R Ab (*right*), or their isotype Abs from the day of zymosan injections (anti–IL-6R isotype: $n = 5$, other groups: $n = 7$). (**C**) H&E stain of the lung from anti–IL-17A Ab (*upper left*), anti–GM-CSF Ab (*upper middle*), anti–IL-6R Ab (*upper right*), or their isotype Abs (*bottom*) injected SKG mouse at 12 wk after zymosan treatment. Scale bar, 500 μm. (**D**) Histological score of anti–IL-17A Ab, anti–GM-CSF Ab, anti–IL-6R Ab, or their isotype Ab injected SKG mice at 12 wk after zymosan treatment (anti–IL-6R isotype: $n = 5$, other groups: $n = 7$). (**E**) The concentrations of pulmonary hydroxyproline in anti–IL-17A Ab, anti–GM-CSF Ab, anti–IL-6R Ab, or their isotype Abs injected SKG mice at 12 wk after zymosan treatment (anti–IL-6R isotype: $n = 5$, other groups: $n = 7$). $^*p < 0.05$, $^{**}p < 0.01$, $^{***}p < 0.001$.

To examine the completeness of IL-17A or GM-CSF neutralization, the serums of Ab-injected mice were diluted to indicated concentrations and added to the 500 pg/ml IL-17A– or GM-CSF–containing sample. The concentration of IL-17A (Supplemental Fig. 4A) and GM-CSF (Supplemental Fig. 4B) in the samples was reduced serum dose dependently and revealed that those serums contained sufficient Abs to neutralize targeted cytokines even at the endpoint. Moreover, the concentration of anti-rat IgG Ab in the serums of anti–GM-CSF Ab or its isotype Ab-injected mice was negligible in most of them (Supplemental Fig. 4C). These data confirmed that IL-17A or GM-CSF neutralization worked completely in this study without induction of Abs against the injected neutralization Abs.

GM-CSF neutralization strongly blocked infiltration of IL-17A– and GM-CSF–producing CD4$^+$ T cells and CD11b$^+$ Gr1$^+$ neutrophils in the lung of zymosan-treated SKG mice

We next measured serum cytokines and fractionations of lung-infiltrating cells of treated mice in Fig. 5. As shown in Fig. 6A, GM-CSF neutralization reduced the serum IFN-γ, IL-17A, IL-6, and TNF-α, but, among them, only IL-6 decreased significantly. In contrast, IL-17A neutralization obviously shut off the serum IL-17A, but serum IL-6 was not decreased. In contrast, by blocking the IL-6 signal, all of these cytokines did not significantly change when compared with its isotype Ab-treated mice. IL-4 and GM-CSF were not detected in all groups (data not shown). These data suggested that IL-17A is dispensable for the progression of this ILD. As shown in Fig. 6B, flow cytometric analysis of infiltrating cells in the lungs revealed significant decrease of total cell counts in anti–GM-CSF Ab-treated mice and relative decrease in anti–IL-6R Ab-treated mice; however, there was no decrease in anti–IL-17A Ab-treated mice. These findings well correlated with the data in Fig. 5. Moreover, GM-CSF neutralization significantly decreased the numbers of infiltrated total CD4$^+$ T cells (especially IL-17A–, GM-CSF–, and IL-6–producing CD4$^+$ T cells), CD11b$^+$ Gr1$^+$ neutrophils, and IL-6–producing CD11b$^+$ Gr1$^-$ macrophages/monocytes. In contrast, blocking of IL-6 signal decreased CD11b$^+$ Gr1$^+$ neutrophils only among these cell populations, and IL-17A neutralization did not decrease any of them. Notably, the number of GM-CSF$^+$ IL-17A$^-$ CD4$^+$ cells, which are major GM-CSF–producing cells, was decreased by GM-CSF neutralization and partly by blocking of IL-6 signal, but that of GM-CSF$^+$ IL-17A$^+$ cells was decreased only by GM-CSF neutralization. These results demonstrated that the most potent molecular target to treat ILD in this mouse was GM-CSF, and that the infiltration of IL-17A–, GM-CSF–producing CD4$^+$ T cells, IL-6–producing CD11b$^+$ Gr1$^-$ macrophages/monocytes, and CD11b$^+$ Gr1$^+$ neutrophils progressed secondary to GM-CSF upregulation in the development of ILD in zymosan-treated SKG mice and can be inhibited by GM-CSF neutralization.

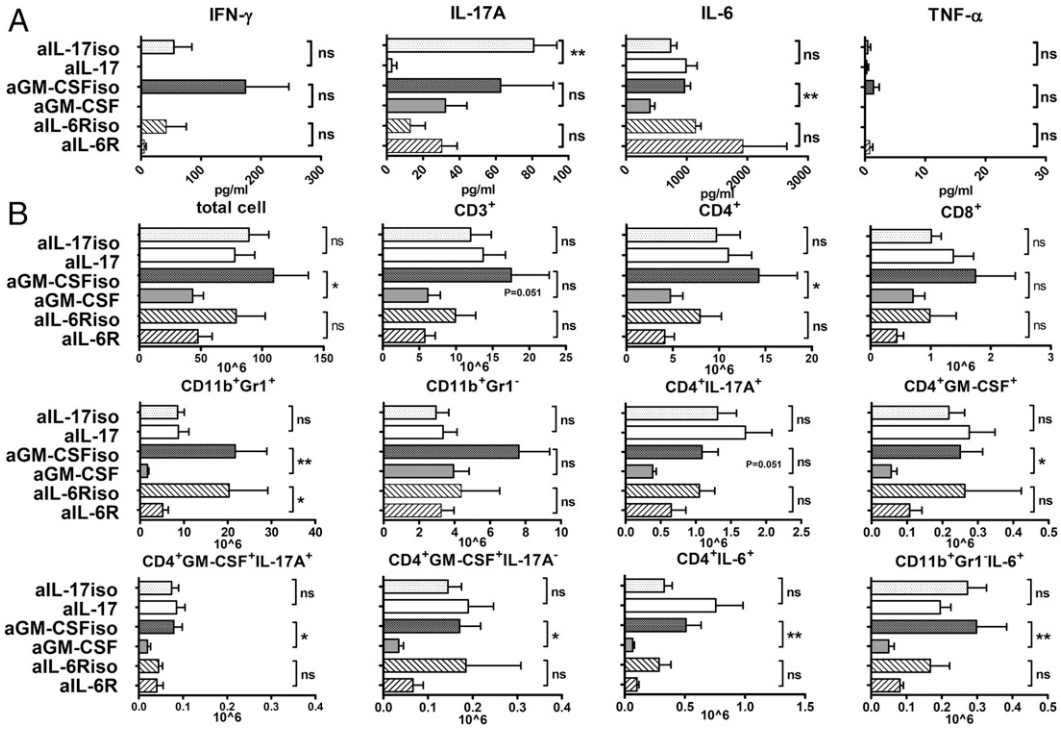

FIGURE 6. GM-CSF neutralization inhibited infiltration of IL-17A$^+$ CD4$^+$ T cells, GM-CSF$^+$ CD4$^+$ T cells, and CD11b$^+$ Gr1$^+$ neutrophils into the lung. (**A**) Serum concentrations of IFN-γ, IL-17A, IL-6, and TNF-α in anti–IL-17A Ab, anti–GM-CSF Ab, anti–IL-6R Ab, or their isotype Abs injected SKG mice at 12 wk after zymosan treatment (anti–IL-6R isotype: $n = 5$, other groups: $n = 7$). (**B**) Infiltrating cell counts in the lungs were measured by flow cytometry of dispersed cells from enzymatic lung digests at 12 wk after zymosan treatment. The numbers of total cells, CD3$^+$ T cells, CD4$^+$ T cells, CD8$^+$ T cells, CD11b$^+$ Gr1$^+$ neutrophils, CD11b$^+$ Gr1$^-$ macrophages/monocytes, IL-17A–producing CD4$^+$ (CD4$^+$ IL-17A$^+$) T cells, GM-CSF–producing CD4$^+$ (CD4$^+$ GM-CSF$^+$) T cells, GM-CSF/IL-17A–double-producing CD4$^+$ (GM-CSF$^+$ IL-17A$^+$ CD4$^+$) T cells, GM-CSF–producing IL-17A–nonproducing CD4$^+$ (GM-CSF$^+$ IL-17A$^-$ CD4$^+$) T cells, IL-6–producing CD4$^+$ (CD4$^+$ IL-6$^+$) T cells, and IL-6–producing macrophages/monocytes (CD11b$^+$ Gr1$^-$ IL-6$^+$) were shown (anti–IL-6R isotype: $n = 5$, other groups: $n = 7$). $*p < 0.05$, $**p < 0.01$.

Treatment by GM-CSF neutralization after the onset of ILD reduced the severity of ILD in zymosan-treated SKG mice

We next analyzed the effect of GM-CSF neutralization after the onset of ILD in zymosan-treated SKG mice. As the histological score of zymosan-treated SKG mice started to increase from the sixth week after zymosan injection (Fig. 1E), each group of SKG mice received six weekly i.p. injections of either anti–GM-CSF Ab or its isotype Ab from the sixth week after zymosan injection. GM-CSF neutralization prevented the weight loss (Fig. 7A) and inhibited the progression of arthritis in zymosan-treated SKG mice (Fig. 7B). Moreover, as shown in Fig. 7C and 7D, GM-CSF neutralization inhibited the progression of ILD in zymosan-treated SKG mice even after the onset of ILD. These results suggested the high potential of GM-CSF neutralization as a therapeutic strategy for severe CTD-ILD in humans (Fig. 8).

Discussion

We described whole features of ILD in zymosan-treated SKG mice and showed that this model is a valuable animal model for CTD-ILD in terms of the chronicity (not self limiting), long time course (5–6 mo), and severity. The most common histological type of CTD-ILD is NSIP (27), and the ILD in this mouse shared many characteristics with NSIP in CTD-ILD in the early phase in terms of the temporally uniform interstitial cellular infiltration and fibrosis, which started in peribronchovascular lesion without honeycombing or fibroblastic foci. Furthermore, it accompanied follicular bronchiolitis, which is one of the characteristics of CTD-ILD (26). Moreover, in the later phase, the ILD in this mouse showed massive infiltration of inflammatory cells within both peribronchiolar and alveolar spaces. It is also known that a combination of different histological patterns and the progressive exacerbation is also pathognomonic and quite frequent in CTD-ILD (27). Therefore, the histological characteristics of ILD in this mouse could be extrapolated to that of severe CTD-ILD. The underlying mechanisms of CTD-ILD development remain poorly understood because of the invasiveness of analyzing procedure such as BAL or open lung biopsy. CD8$^+$ T cells (30, 31), as well as some subtypes of CD4$^+$ T cells, including Th2, regulatory T cells, and Th17 cells (32, 33), and neutrophils (5–8) are reported as contributors of pulmonary fibrosis. However, in contrast with idiopathic pulmonary fiborosis, CTD-ILD is often characterized by a clearer response to immunosuppression, indicating that autoimmune/inflammatory mechanisms play a more significant and central role than fibrosis in CTD-ILD pathogenesis (27, 34). Analyses of alveolitis using BAL fluid showed accumulation of neutrophils with or without increased percentages of T cells in the small airways of CTD-ILD (4, 5), and neutrophils were reported as important effector cells and associated with poor outcome of CTD-ILD (5–8). The CD4/CD8 ratios in BAL fluid of CTD-ILD patients vary with reports (30, 35–39); however, a previous report showed that correlation between CD4/CD8 ratios in lung tissue and CD4/CD8 ratios in BAL fluid was weak and that CD4/CD8 ratio in BAL fluid would rather reflect the extent of fibrosis (40). In contrast, in histological analyses, increased number of CD4$^+$ T cells in lung tissue of open lung biopsy was reported as characteristics of CTD-ILD (9). Previous reports showed that CD4$^+$ T cells and B cells were observed inside and around lymphoid follicles and in the thick fibrotic wall of reconstructed alveoli with fibrosis, and CD8$^+$ T cells were diffusely distributed especially in

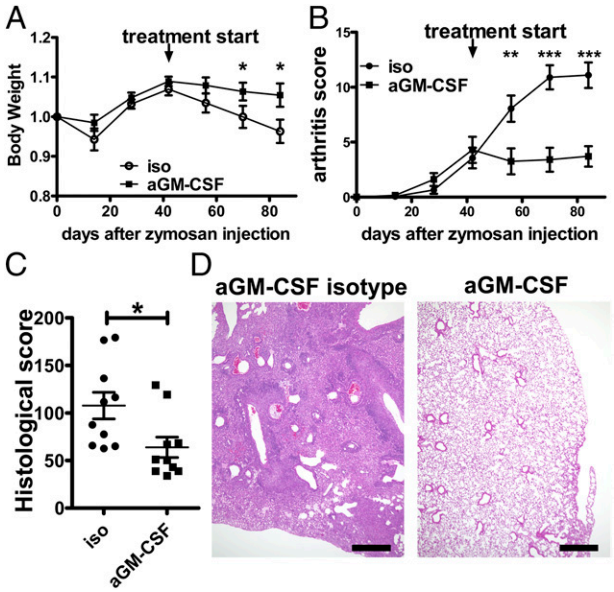

FIGURE 7. GM-CSF neutralization inhibited the progression of ILD even after the onset of ILD. (**A** and **B**) Weight change ratio (A) and arthritis score (B) of SKG mice that received a single i.p. injection of zymosan followed by six weekly i.p. injections of anti–GM-CSF Ab (*left*) or its isotype Ab from the sixth week after zymosan injections (n = 10). (**C**) Histological scores of SKG mice given six anti–GM-CSF Ab or isotype Ab weekly injections at 12 wk after zymosan injection (n = 10). (**D**) H&E stain of the lung from SKG mouse given six anti–GM-CSF Ab (*right*) or its isotype Ab (*left*) weekly injections at 12 wk after zymosan injection. Scale bar, 500 μm. $*p < 0.05$, $**p < 0.01$, $***p < 0.001$.

relatively thin alveoli in CTD-ILD patients, suggesting that $CD4^+$ and B cells initiate and operate cell-mediated humoral and immune mechanisms and $CD8^+$ T cells and neutrophils cause lung injury in the CTD-ILD (37, 40). By cytological analysis, ILD in SKG mice was characterized by the increased infiltration of $CD4^+$ T cells and neutrophils. Therefore, these data also indicated the similarity of CTD-ILD and ILD in zymosan-treated SKG mice and that $CD4^+$ T cells as well as neutrophils are critical for the development of both of them. Therefore, ILD in this mouse can be a suitable model of severe CTD-ILD and is very useful to analyze the mechanisms and the effects of the therapeutic interventions to treat them.

SKG arthritis is known to be mediated by Th17 cells (13), but the mechanisms underlying the progression of ILD are yet to be clarified. In this study, we showed that high potential of SKG T cells to produce GM-CSF produced a different outcome between zymosan-treated SKG and BALB/c. GM-CSF was reported to upregulate TLR2, TLR4, and CD14 expression (41–43) and boost IL-6 and IL-1β production from macrophages (41, 44, 45). Although serum concentration of GM-CSF in zymosan-treated SKG mice was very low and could not be detected by ELISA, we showed that GM-CSF could enhance the production of IL-6 and IL-1β by macrophages even at a low concentration (Fig. 3). In addition, GM-CSF itself is a strong inducer of neutrophil infiltration (46). Previous reports showed that overexpression of GM-CSF led to severe neutrophil and macrophage infiltration in multiple tissues, including lung (47), and, as we showed, GM-CSF neutralization significantly inhibited the neutrophil infiltration into the lung of zymosan-treated SKG mice (Fig. 6B). These results indicated that GM-CSF essentially contributed to the progression of ILD in zymosan-treated SKG mice both directly and indirectly.

GM-CSF is known as one of the Th17 cytokines; however, it is not exclusively produced by Th17 cells, but also by other T cell subsets, including $CD8^+$ T cells. The number of GM-CSF–producing $CD8^+$ T cells also increased in both zymosan-treated BALB/c and zymosan-treated SKG mice (Supplemental Fig. 4D). However, the contribution of GM-CSF–producing $CD8^+$ T cells to the development of ILD seems to be small, for the number of GM-CSF–producing $CD8^+$ T cells is about one-tenth of that of GM-CSF–producing $CD4^+$ T cells (Fig. 2C) in zymosan-treated SKG mice and is equivalent to that in zymosan-treated BALB/c mice. These results reinforced that GM-CSF^+ IL-$17A^-$ $CD4^+$ T cells are main effector cells in this model.

IL-17A is also known as a strong inducer of neutrophil infiltration (48), but IL-17A neutralization was not effective to prevent ILD in this mouse. Considering the previous report that no morphological change was found in the lungs of IL-17–overexpressing mice (49) and that serum IL-17A was almost completely diminished in anti–IL-17A–injected group and was not in anti–GM-CSF Ab- or anti–IL-6R Ab-injected group, IL-17A seemed not to be essential for the development of this ILD. In addition, there was

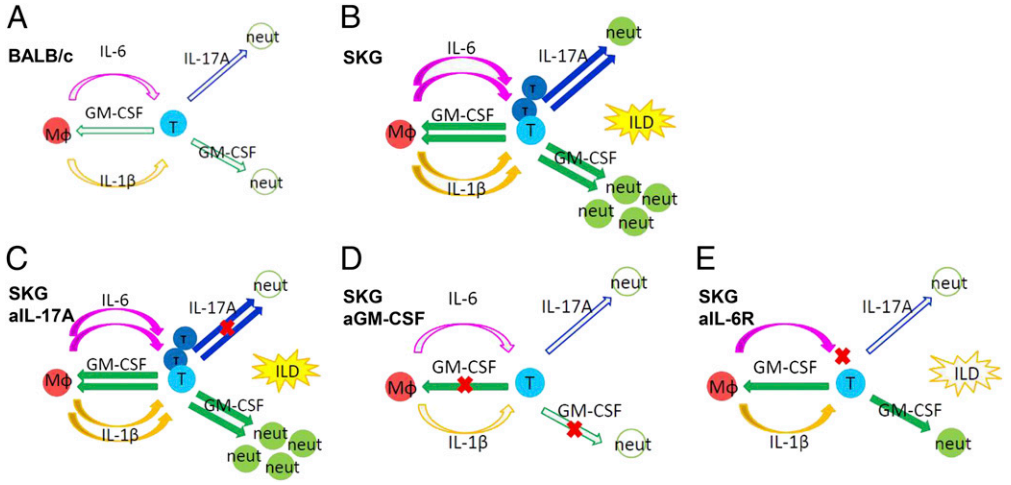

FIGURE 8. Models of the role of GM-CSF in the development of ILD in SKG mice. (**A**) T cells of zymosan-treated BALB/c mice produce lower amount of GM-CSF or IL-17A in response to macrophage stimulation, and the vicious circle of IL-17A– and GM-CSF–producing T cell expansion is not exacerbated. (**B**) T cells of zymosan-treated SKG mice preferentially produce higher amount of GM-CSF, which stimulates cytokine production of macrophages, and resulted in exacerbation of vicious circle of IL-17A– and GM-CSF–producing T cell expansion. (**C**–**E**) A model of IL-17A neutralization (C), GM-CSF neutralization (D), and anti–IL-6R Ab (E) treatment in zymosan-treated SKG mice.

no difference between zymosan-treated BALB/c and zymosan-treated SKG mice in the serum IL-17AF heterodimer or IL-17F homodimer, the other IL-17 family members secreted by $CD4^+$ T cells and having similar function (48) (Supplemental Fig. 4E), indicating they are not important to the pathogenesis of this ILD either.

By contrast, anti–IL-6R Ab treatment resulted in partial amelioration of ILD in this mouse. Blocking of IL-6 signal reduced the number of GM-CSF^+ IL-$17A^-$ $CD4^+$ T cells to some extent but not that of GM-CSF^+ IL-$17A^+$ $CD4^+$ T cells, although GM-CSF neutralization reduced both of them (Fig. 6B). These differences may be the cause of partial inhibition of ILD by blocking of IL-6 signal. In addition, considering that anti–IL-6R Ab or its isotype Ab-injected mice received higher amount of Ig than anti–IL-17A or anti–GM-CSF Ab-injected groups, higher Ig dosages themselves may have some curative effects as reported effect of high-dose i.v. Ig therapy (50). In fact, the severity of ILD and weight loss in the isotype Ab of anti–IL-6R–treated group seemed milder than that of anti–IL-17A isotype or anti–GM-CSF isotype Ab-treated groups, although there was no statistical difference (Fig. 5A, 5D, 5E, Supplemental Fig. 3).

In summary, we found that GM-CSF plays a key role by enhancing IL-6 and IL-1β production from zymosan-activated macrophages to promote the differentiation of IL-17A– or GM-CSF–producing T cells. Moreover, GM-CSF enhances granulopoiesis and neutrophil infiltration (Fig. 8A, 8B). Therefore, GM-CSF neutralization strongly inhibited the progression of ILD in this mouse by blocking both positive feedback loop of IL-17A– and GM-CSF–producing T cell differentiation and the neutrophil infiltration induced by GM-CSF itself (Fig. 8D). IL-17A neutralization failed to ameliorate this ILD, indicating that IL-17A is not a key molecule to the progression of this ILD (Fig. 8C). Blocking of IL-6 signal resulted in partial inhibition of this ILD, indicating that it partially suppressed the differentiation of IL-17– and GM-CSF–producing T cells, and then neutrophil infiltration in lung (Fig. 8E).

It is known that auto-Ab to GM-CSF is responsible for the development of pulmonary alveolar proteinosis (PAP) (51), and GM-CSF–deficient mice develop abnormal lung virtually indistinguishable from human PAP (52). However, only trace amounts of GM-CSF are needed for lung homeostasis, and neutralizing GM-CSF with Abs in mice has no demonstrated adverse reactions, indicating its wide therapeutic index (53). In fact, there was no evidence for alveolar proteinosis in anti–GM-CSF Ab-treated mice such as foamy alveolar macrophages in a distinctive background of eosinophilic, granular, periodic acid-Schiff positive material filling alveoli (51) (Supplemental Fig. 4F). Therefore, neutralization/blocking Abs are a useful approach and can easily receive clinical applications. Now, Mavrilimumab, anti–GM-CSF receptor α Ab, is being developed, and a phase II study in subjects with rheumatoid arthritis patients is reported to have significant efficacy and no serious adverse events, including PAP (54). Regarding the fact that neutralization of GM-CSF ameliorated ILD in SKG mice even after the onset of ILD, it can provide a useful therapeutic strategy in CTD-ILD in humans.

In conclusion, we described that zymosan-treated SKG mice develop chronic–progressive and lethal ILD over several months, and ILD of this mouse shared many characteristics with severe CTD-ILD. Therefore, this ILD might be a useful mouse model for elucidating the underlying mechanism and devising effective treatment of severe CTD-ILD. Furthermore, we found that GM-CSF played a pivotal role in the pathogenesis of ILD in this mouse, and that neutralization of GM-CSF has great therapeutic potential. Because it is almost impossible to examine the pathology in life-threatening severe CTD-ILD in humans, further elucidation of the molecular mechanisms of ILD in this mouse would help in devising preventive or curative strategies for it.

Acknowledgments

We thank Kensaku Aihara (Department of Respiratory Medicine, Graduate School of Medicine, Kyoto University) for technical support on hydroxyproline measurement, Aya Miyagawa-Hayashino (Department of Diagnostic Pathology, Kyoto University Hospital) for pathological evaluation, and Sonoko Nagai (Department of Respiratory Medicine, Graduate School of Medicine, Kyoto University) for critical reading.

Disclosures

The authors have no financial conflicts of interest.

References

1. Castelino, F. V., and J. Varga. 2010. Interstitial lung disease in connective tissue diseases: evolving concepts of pathogenesis and management. *Arthritis Res. Ther.* 12: 213.
2. Katzenstein, A. L., and J. L. Myers. 1998. Idiopathic pulmonary fibrosis: clinical relevance of pathologic classification. *Am. J. Respir. Crit. Care Med.* 157: 1301–1315.
3. Parra, E. R., G. S. Noleto, L. J. Tinoco, and V. L. Capelozzi. 2008. Immunophenotyping and remodeling process in small airways of idiopathic interstitial pneumonias: functional and prognostic significance. *Clin. Respir. J.* 2: 227–238.
4. Wallaert, B. 1990. Subclinical alveolitis in immunologic systemic disorders. *Lung* 168: 974–983.
5. Manganelli, P., F. Salaffi, and A. Pesci. 1997. Clinical and subclinical alveolitis in connective tissue diseases assessed by bronchoalveolar lavage. *Semin. Arthritis Rheum.* 26: 740–754.
6. Garcia, J. G., N. Parhami, D. Killam, P. L. Garcia, and B. A. Keogh. 1986. Bronchoalveolar lavage fluid evaluation in rheumatoid arthritis. *Am. Rev. Respir. Dis.* 133: 450–454.
7. Garcia, J. G., H. L. James, S. Zinkgraf, M. B. Perlman, and B. A. Keogh. 1987. Lower respiratory tract abnormalities in rheumatoid interstitial lung disease: potential role of neutrophils in lung injury. *Am. Rev. Respir. Dis.* 136: 811–817.
8. Marie, I., E. Hachulla, P. Chérin, S. Dominique, P. Y. Hatron, M. F. Hellot, B. Devulder, S. Herson, H. Levesque, and H. Courtois. 2002. Interstitial lung disease in polymyositis and dermatomyositis. *Arthritis Rheum.* 47: 614–622.
9. Turesson, C., E. L. Matteson, T. V. Colby, Z. Vuk-Pavlovic, R. Vassallo, C. M. Weyand, H. D. Tazelaar, and A. H. Limper. 2005. Increased CD4+ T cell infiltrates in rheumatoid arthritis-associated interstitial pneumonitis compared with idiopathic interstitial pneumonitis. *Arthritis Rheum.* 52: 73–79.
10. Moore, B., W. E. Lawson, T. D. Oury, T. H. Sisson, K. Raghavendran, and C. M. Hogaboam. 2013. Animal models of fibrotic lung disease. *Am. J. Respir. Cell Mol. Biol.* 49: 167–179.
11. Sakaguchi, N., T. Takahashi, H. Hata, T. Nomura, T. Tagami, S. Yamazaki, T. Sakihama, T. Matsutani, I. Negishi, S. Nakatsuru, and S. Sakaguchi. 2003. Altered thymic T-cell selection due to a mutation of the ZAP-70 gene causes autoimmune arthritis in mice. *Nature* 426: 454–460.
12. Keith, R. C., J. L. Powers, E. F. Redente, A. Sergew, R. J. Martin, A. Gizinski, V. M. Holers, S. Sakaguchi, and D. W. Riches. 2012. A novel model of rheumatoid arthritis-associated interstitial lung disease in SKG mice. *Exp. Lung Res.* 38: 55–66.
13. Hirota, K., M. Hashimoto, H. Yoshitomi, S. Tanaka, T. Nomura, T. Yamaguchi, Y. Iwakura, N. Sakaguchi, and S. Sakaguchi. 2007. T cell self-reactivity forms a cytokine milieu for spontaneous development of IL-17+ Th cells that cause autoimmune arthritis. *J. Exp. Med.* 204: 41–47.
14. Yoshitomi, H., N. Sakaguchi, K. Kobayashi, G. D. Brown, T. Tagami, T. Sakihama, K. Hirota, S. Tanaka, T. Nomura, I. Miki, et al. 2005. A role for fungal beta-glucans and their receptor Dectin-1 in the induction of autoimmune arthritis in genetically susceptible mice. *J. Exp. Med.* 201: 949–960.
15. Hashimoto, M., K. Hirota, H. Yoshitomi, S. Maeda, S. Teradaira, S. Akizuki, P. Prieto-Martin, T. Nomura, N. Sakaguchi, J. Köhl, et al. 2010. Complement drives Th17 cell differentiation and triggers autoimmune arthritis. *J. Exp. Med.* 207: 1135–1143.
16. Zhang, Y., G. Ren, M. Guo, X. Ye, J. Zhao, L. Xu, J. Qi, F. Kan, M. Liu, and D. Li. 2013. Synergistic effects of interleukin-1β and interleukin-17A antibodies on collagen-induced arthritis mouse model. *Int. Immunopharmacol.* 15: 199–205.
17. van den Berg, W. B., and I. B. McInnes. 2013. Th17 cells and IL-17 a—focus on immunopathogenesis and immunotherapeutics. *Semin. Arthritis Rheum.* 43: 158–170.
18. Nakae, S., A. Nambu, K. Sudo, and Y. Iwakura. 2003. Suppression of immune induction of collagen-induced arthritis in IL-17-deficient mice. *J. Immunol.* 171: 6173–6177.
19. Codarri, L., G. Gyülvészi, V. Tosevski, L. Hesske, A. Fontana, L. Magnenat, T. Suter, and B. Becher. 2011. RORγt drives production of the cytokine GM-CSF in helper T cells, which is essential for the effector phase of autoimmune neuroinflammation. *Nat. Immunol.* 12: 560–567.

20. El-Behi, M., B. Ciric, H. Dai, Y. Yan, M. Cullimore, F. Safavi, G. X. Zhang, B. N. Dittel, and A. Rostami. 2011. The encephalitogenicity of T(H)17 cells is dependent on IL-1- and IL-23-induced production of the cytokine GM-CSF. *Nat. Immunol.* 12: 568–575.
21. Ye, P., W. Chen, J. Wu, X. Huang, J. Li, S. Wang, Z. Liu, G. Wang, X. Yang, P. Zhang, et al. 2013. GM-CSF contributes to aortic aneurysms resulting from SMAD3 deficiency. *J. Clin. Invest.* 123: 2317–2331.
22. Wakasa-Morimoto, C., T. Toyosaki-Maeda, T. Matsutani, R. Yoshida, S. Nakamura-Kikuoka, M. Maeda-Tanimura, H. Yoshitomi, K. Hirota, M. Hashimoto, H. Masaki, et al. 2008. Arthritis and pneumonitis produced by the same T cell clones from mice with spontaneous autoimmune arthritis. *Int. Immunol.* 20: 1331–1342.
23. Nishikomori, R., R. O. Ehrhardt, and W. Strober. 2000. T helper type 2 cell differentiation occurs in the presence of interleukin 12 receptor beta2 chain expression and signaling. *J. Exp. Med.* 191: 847–858.
24. Frankel, S. K., B. M. Moats-Staats, C. D. Cool, M. W. Wynes, A. D. Stiles, and D. W. Riches. 2005. Human insulin-like growth factor-IA expression in transgenic mice promotes adenomatous hyperplasia but not pulmonary fibrosis. *Am. J. Physiol. Lung Cell. Mol. Physiol.* 288: L805–L812.
25. Yoshida, H., M. Hashizume, M. Suzuki, and M. Mihara. 2011. Induction of high-dose tolerance to the rat anti-mouse IL-6 receptor antibody in NZB/NZW F1 mice. *Rheumatol. Int.* 31: 1445–1449.
26. Tansey, D., A. U. Wells, T. V. Colby, S. Ip, A. Nikolakoupolou, R. M. du Bois, D. M. Hansell, and A. G. Nicholson. 2004. Variations in histological patterns of interstitial pneumonia between connective tissue disorders and their relationship to prognosis. *Histopathology* 44: 585–596.
27. de Lauretis, A., S. Veeraraghavan, and E. Renzoni. 2011. Review series: aspects of interstitial lung disease: connective tissue disease-associated interstitial lung disease: how does it differ from IPF? How should the clinical approach differ? *Chron. Respir. Dis.* 8: 53–82.
28. Bondeson, J., K. A. Browne, F. M. Brennan, B. M. Foxwell, and M. Feldmann. 1999. Selective regulation of cytokine induction by adenoviral gene transfer of IkappaBalpha into human macrophages: lipopolysaccharide-induced, but not zymosan-induced, proinflammatory cytokines are inhibited, but IL-10 is nuclear factor-kappaB independent. *J. Immunol.* 162: 2939–2945.
29. Lukens, J. R., M. J. Barr, D. D. Chaplin, H. Chi, and T. D. Kanneganti. 2012. Inflammasome-derived IL-1β regulates the production of GM-CSF by CD4(+) T cells and γδ T cells. *J. Immunol.* 188: 3107–3115.
30. Atamas, S. P., V. V. Yurovsky, R. Wise, F. M. Wigley, C. J. Goter Robinson, P. Henry, W. J. Alms, and B. White. 1999. Production of type 2 cytokines by CD8+ lung cells is associated with greater decline in pulmonary function in patients with systemic sclerosis. *Arthritis Rheum.* 42: 1168–1178.
31. Luzina, I. G., S. P. Atamas, R. Wise, F. M. Wigley, J. Choi, H. Q. Xiao, and B. White. 2003. Occurrence of an activated, profibrotic pattern of gene expression in lung CD8+ T cells from scleroderma patients. *Arthritis Rheum.* 48: 2262–2274.
32. Luzina, I. G., N. W. Todd, A. T. Iacono, and S. P. Atamas. 2008. Roles of T lymphocytes in pulmonary fibrosis. *J. Leukoc. Biol.* 83: 237–244.
33. Lo Re, S., D. Lison, and F. Huaux. 2013. CD4+ T lymphocytes in lung fibrosis: diverse subsets, diverse functions. *J. Leukoc. Biol.* 93: 499–510.
34. Vij, R., and M. E. Strek. 2013. Diagnosis and treatment of connective tissue disease-associated interstitial lung disease. *Chest* 143: 814–824.
35. Shimizu, Y., H. Kuwabara, A. Ono, S. Higuchi, T. Hisada, K. Dobashi, M. Utsugi, Y. Mita, and M. Mori. 2006. Intracellular Th1/Th2 balance of pulmonary CD4(+) T cells in patients with active interstitial pneumonia evaluated by serum KL-6. *Immunopharmacol. Immunotoxicol.* 28: 295–304.
36. Kolarz, G., O. Scherak, W. Popp, L. Ritschka, N. Thumb, A. Wottawa, and H. Zwick. 1993. Bronchoalveolar lavage in rheumatoid arthritis. *Br. J. Rheumatol.* 32: 556–561.
37. Nagasawa, Y., T. Takada, T. Shimizu, J. Narita, H. Moriyama, M. Terada, E. Suzuki, and F. Gejyo. 2009. Inflammatory cells in lung disease associated with rheumatoid arthritis. *Intern. Med.* 48: 1209–1217.
38. Enomoto, K., T. Takada, E. Suzuki, T. Ishida, H. Moriyama, H. Ooi, T. Hasegawa, H. Tsukada, M. Nakano, and F. Gejyo. 2003. Bronchoalveolar lavage fluid cells in mixed connective tissue disease. *Respirology* 8: 149–156.
39. Sauty, A., T. Rochat, O. D. Schoch, J. Hamacher, A. M. Kurt, J. M. Dayer, and L. P. Nicod. 1997. Pulmonary fibrosis with predominant CD8 lymphocytic alveolitis and anti-Jo-1 antibodies. *Eur. Respir. J.* 10: 2907–2912.
40. Yamadori, I., J. Fujita, H. Kajitani, S. Bandoh, M. Tokuda, Y. Yang, Y. Ohtsuki, T. Yoshinouchi, T. Kamei, and T. Ishida. 2000. Lymphocyte subsets in lung tissues of non-specific interstitial pneumonia and pulmonary fibrosis associated with collagen vascular disorders: correlation with CD4/CD8 ratio in bronchoalveolar lavage. *Lung* 178: 361–370.
41. Parajuli, B., Y. Sonobe, J. Kawanokuchi, Y. Doi, M. Noda, H. Takeuchi, T. Mizuno, and A. Suzumura. 2012. GM-CSF increases LPS-induced production of proinflammatory mediators via upregulation of TLR4 and CD14 in murine microglia. *J. Neuroinflammation* 9: 268.
42. Sorgi, C. A., S. Rose, N. Court, D. Carlos, F. W. Paula-Silva, P. A. Assis, F. G. Frantz, B. Ryffel, V. Quesniaux, and L. H. Faccioli. 2012. GM-CSF priming drives bone marrow-derived macrophages to a pro-inflammatory pattern and downmodulates PGE2 in response to TLR2 ligands. *PLoS One* 7: e40523.
43. Berclaz, P. Y., B. Carey, M. D. Fillipi, K. Wernke-Dollries, N. Geraci, S. Cush, T. Richardson, J. Kitzmiller, M. O'Connor, C. Hermoyian, et al. 2007. GM-CSF regulates a PU.1-dependent transcriptional program determining the pulmonary response to LPS. *Am. J. Respir. Cell Mol. Biol.* 36: 114–121.
44. Sonderegger, I., G. Iezzi, R. Maier, N. Schmitz, M. Kurrer, and M. Kopf. 2008. GM-CSF mediates autoimmunity by enhancing IL-6-dependent Th17 cell development and survival. *J. Exp. Med.* 205: 2281–2294.
45. Khameneh, H. J., S. A. Isa, L. Min, F. W. Nih, and C. Ruedl. 2011. GM-CSF signalling boosts dramatically IL-1 production. *PLoS One* 6: e23025.
46. Shi, Y., C. H. Liu, A. I. Roberts, J. Das, G. Xu, G. Ren, Y. Zhang, L. Zhang, Z. R. Yuan, H. S. Tan, et al. 2006. Granulocyte-macrophage colony-stimulating factor (GM-CSF) and T-cell responses: what we do and don't know. *Cell Res.* 16: 126–133.
47. Johnson, G. R., T. J. Gonda, D. Metcalf, I. K. Hariharan, and S. Cory. 1989. A lethal myeloproliferative syndrome in mice transplanted with bone marrow cells infected with a retrovirus expressing granulocyte-macrophage colony stimulating factor. *EMBO J.* 8: 441–448.
48. Kolls, J. K., and A. Lindén. 2004. Interleukin-17 family members and inflammation. *Immunity* 21: 467–476.
49. Tang, H., S. Pang, M. Wang, X. Xiao, Y. Rong, H. Wang, and Y. Q. Zang. 2010. TLR4 activation is required for IL-17-induced multiple tissue inflammation and wasting in mice. *J. Immunol.* 185: 2563–2569.
50. Spurlock, N. K., and J. E. Prittie. 2011. A review of current indications, adverse effects, and administration recommendations for intravenous immunoglobulin. *J. Vet. Emerg. Crit. Care* 21: 471–483.
51. Greenhill, S. R., and D. N. Kotton. 2009. Pulmonary alveolar proteinosis: a bench-to-bedside story of granulocyte-macrophage colony-stimulating factor dysfunction. *Chest* 136: 571–577.
52. Dranoff, G., A. D. Crawford, M. Sadelain, B. Ream, A. Rashid, R. T. Bronson, G. R. Dickersin, C. J. Bachurski, E. L. Mark, J. A. Whitsett, et al. 1994. Involvement of granulocyte-macrophage colony-stimulating factor in pulmonary homeostasis. *Science* 264: 713–716.
53. Vlahos, R., S. Bozinovski, J. A. Hamilton, and G. P. Anderson. 2006. Therapeutic potential of treating chronic obstructive pulmonary disease (COPD) by neutralising granulocyte macrophage-colony stimulating factor (GM-CSF). *Pharmacol. Ther.* 112: 106–115.
54. Burmester, G. R., M. E. Weinblatt, I. B. McInnes, D. Porter, O. Barbarash, M. Vatutin, I. Szombati, E. Esfandiari, M. A. Sleeman, and C. D. Kane, et al. 2013. Efficacy and safety of mavrilimumab in subjects with rheumatoid arthritis. *Ann. Rheum. Dis.* 72: 1445-1452.

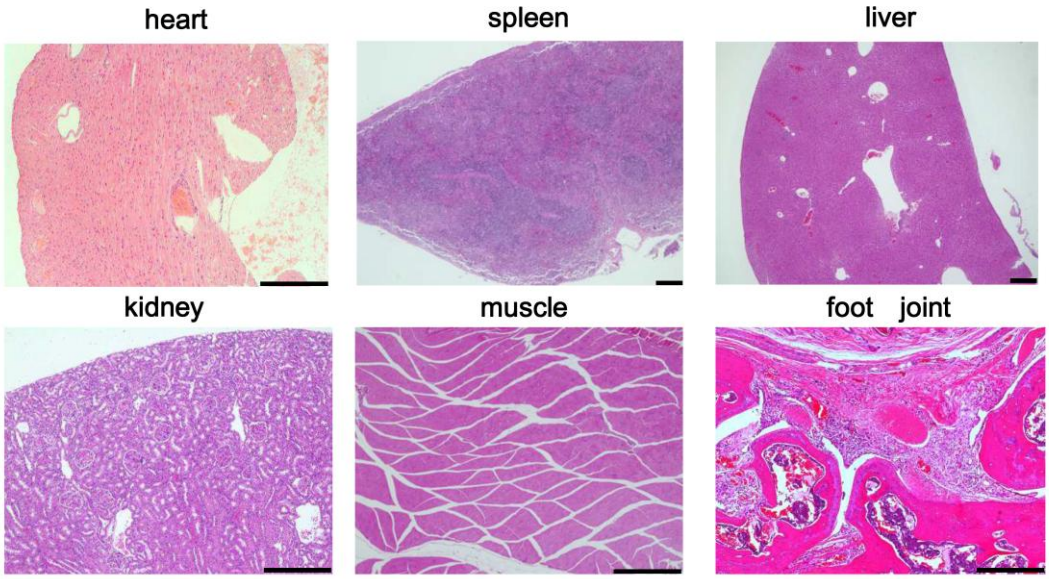

Supplemental Figure 1. Histology of zymosan-treated SKG mice.

Histology of the internal organs of zymosan-treated SKG mice. Infiltration of inflammatory cells in organs was mild except for foot joint in zymosan-treated SKG mice. H&E stain. Bar = 300μm

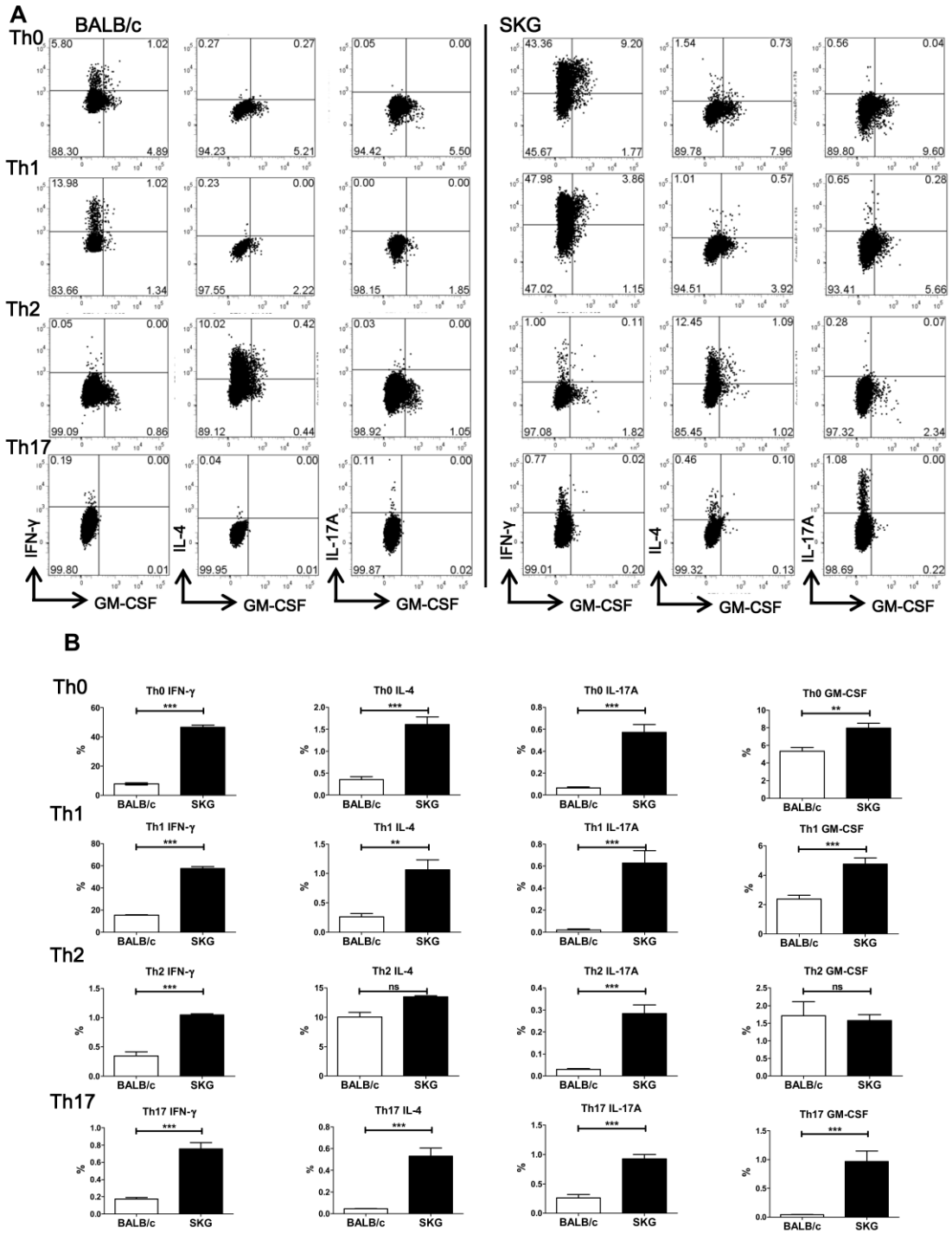

Supplemental Figure 2. SKG $CD4^+$ T cells were skewed to differentiate into IL-17A- or GM-CSF-producing cells.

A and B, FACS sorted $CD4^+$ $CD62L^+$ naïve T cells of SKG and BALB/c mice were

stimulated with anti-CD3/28 Abs under neutral (Th0) conditions, Th1 conditions (IL-12, anti-IL-4 Ab), Th2 conditions (IL-4, anti-IFN-γ Ab), and Th17 conditions (IL-6, TGF-β, anti-IFN-γ Ab). At day 5, cultured cells were analyzed by FACS. Representative results were shown in (A) and overall results were summarized in (B) (n=6).

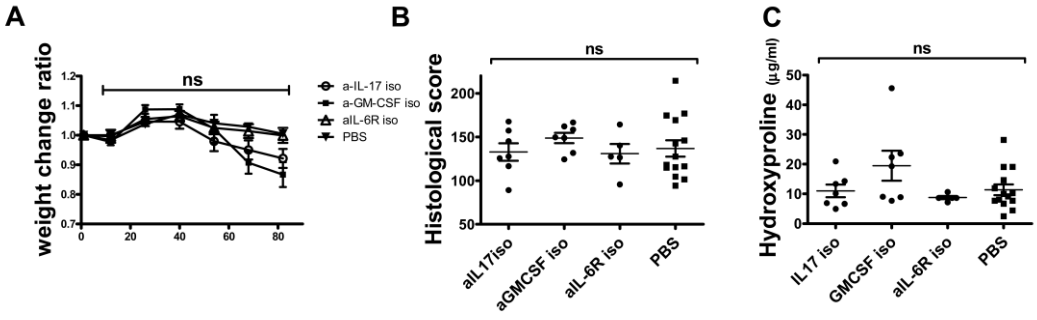

Supplemental Figure 3. Isotype control antibodies are not pathogenic on its own.

A, Weight change ratio of SKG mice that received a single i.p. injection of zymosan and 12 times of weekly i.p. injection of anti-IL-17A isotype, anti-GM-CSF isotype, anti-IL-6R isotype antibodies or PBS from the day of zymosan injection (PBS: n=14, anti-IL-6R isotype: n=5, other groups: n=7). There was no statistical difference among these 4 groups.

B, Histological score of weekly anti-IL-17A isotype, anti-GM-CSF isotype, anti-IL-6R isotype antibodies or PBS injected SKG mice at 12 weeks after zymosan treatment (PBS: n=14, anti-IL-6R isotype: n=5, other groups: n=7). There was no statistical difference among these 4 groups.

C, The concentrations of pulmonary hydroxyproline of weekly anti-IL-17A isotype, anti-GM-CSF isotype, anti-IL-6R isotype antibodies or PBS injected SKG mice at 12 weeks after zymosan treatment (PBS: n=14, anti-IL-6R isotype: n=5, other groups: n=7). There was no statistical difference among these 4 groups.

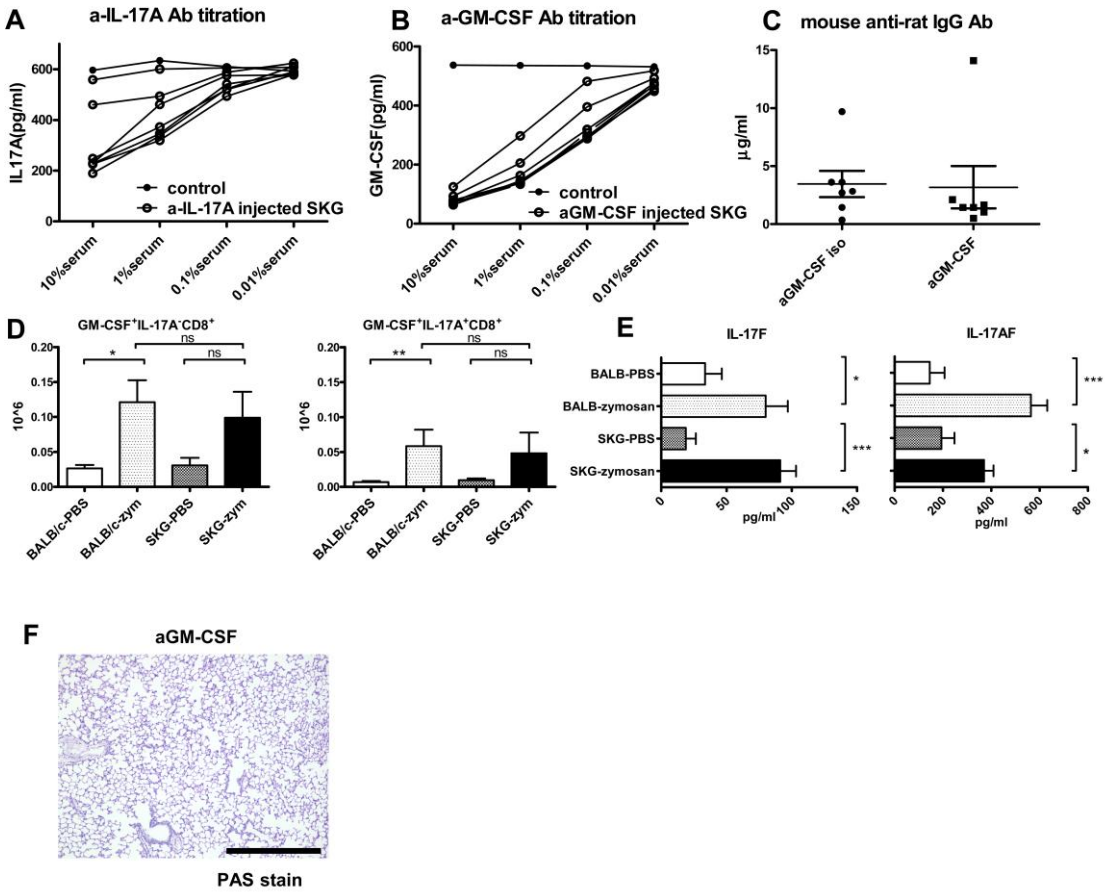

Supplemental Figure 4. Profiles of lung infiltrating cells and serum cytokines in zymosan-treated mice.

A and B, Sufficient antibodies to neutralize IL-17A or GM-CSF were remaining in the sera of anti-IL-17A or anti-GM-CSF antibody injected SKG mice at the point of sacrifice. The serum of anti-IL-17A antibody injected mice (A), anti-GM-CSF antibody injected mice (B), or non-treated control mice were diluted to indicated concentrations and added to the 500 pg/ml IL-17A (A) or GM-CSF (B) containing sample. The concentrations of IL-17A (A) and GM-CSF (B) were measured by ELISA (n=7).

C, The concentrations of mouse anti-rat IgG antibodies in the sera of anti-GM-CSF antibody or its isotype antibody injected mice were measured by ELISA (n=7).

D, The number of GM-CSF$^+$IL-17A$^+$CD8$^+$ T cells and that of GM-CSF$^+$IL-17A$^-$CD8$^+$ T cells in the lung of zymosan- or PBS-treated SKG and BALB/c mice in Fig. 2. Infiltrating cell counts in lungs were measured by Flow cytometry of dispersed cells from enzymatic lung digests.

E, Serum concentration of IL-17F, IL-17AF in zymosan- or PBS-treated BALB/c and SKG mice in Fig. 2. (PBS: n=5, zymosan: n=15)

F, Representative PAS stain of the lung from anti-GM-CSF antibody injected SKG mouse in Fig.5. No foamy alveolar macrophages or PAS positive material filling alveoli were observed. Bar = 500 μm